

Optical Torques in Suspended Fabry-Perot Interferometers

John A. Sidles

University of Washington, School of Medicine, Box 356500, Seattle, Washington, 98195, USA

Daniel Sigg

LIGO Hanford Observatory, P.O. Box 159, Richland, WA 99352, USA

Abstract

High-power Fabry-Perot cavities with suspended mirrors are employed in gravitational wave detection. The mirrors in such interferometers are subject to forces and torques that are exerted by light pressure. This article derives a closed-form expression for the static torsional stiffness due to this effect. The torsional stiffness is shown to scale as the fourth power of the beam spot size. In proposed designs for next-generation interferometric gravitational wave detectors the torsional stiffness is shown to be large enough to dominate the dynamics of the mirror suspensions.

Key words: Fabry-Perot, optomechanical, torque, torsion, mirrors

PACS: 07.60.Ly, 04.80.Nn, 95.55.Ym

1 Introduction

The suspended mirrors in interferometric gravitational wave interferometers form Fabry-Perot cavities in the Michelson arms, subject to high optical powers. Angular mirror motions cause the optical axis to wander off-center, such that radiation pressure then exerts torque upon the mirrors. In this article we calculate the torsional stiffness resulting from this effect.

Our analysis is based on virtual work principles and simple geometric considerations. We consider only the quasi-static limit of the optical forces and

Email addresses: sidles@u.washington.edu (John A. Sidles),
sigg_d@ligo.caltech.edu (Daniel Sigg).

torques, that is, we consider only mirror motions that are slow compared to the ringdown time of the optical cavity. We show that in this limit the torsional stiffness is determined entirely by the geometric figure of the cavity, specifically via the g_1 and g_2 mirror parameters. We construct the stiffness matrix for coupled translations and rotations of the two mirrors, and we show that this matrix has a simple and physically illuminating analytic form.

The existence and importance of optically-generated torques was first recognized in a 1991 article by Solimeno *et al.* [1]. Their analysis employed a sophisticated modal formalism. We will show that the modal and geometric formalisms agree perfectly when they overlap.

However, the complexity of the modal formalism has obscured what a geometric analysis makes evident: in high-power interferometry the optically-induced torsional stiffness can be large enough to overwhelm the stiffness of the mirror suspension. Furthermore, we show that a suspended-mirror cavity always has one torsional mode that is statically unstable. We show that the unstable torsional stiffness can be minimized by choosing negative g -parameters for the cavity mirrors. And finally, we show that increasing the beam diameter—in order to minimize thermoelastic noise [2,3]—is necessarily accompanied by an increase in the torsional coupling.

These findings illustrate that in high-power interferometry there are important design challenges and dependencies between the optical cavity design, the mirror suspension design and the sensing and control design.

2 Conventions

In describing mirror displacements, we assign to each mirror a right-handed set of mirror-specific *basis vectors* $\{\hat{\mathbf{x}}, \hat{\mathbf{y}}, \hat{\mathbf{z}}\}$. These vectors have unit length, and in accord with common usage they are defined to be:

$$\hat{\mathbf{z}} \equiv \text{normal to the reflecting surface}, \quad (1a)$$

$$\hat{\mathbf{y}} \equiv \text{vertical with respect to the floor}, \quad (1b)$$

$$\hat{\mathbf{x}} \equiv \hat{\mathbf{y}} \times \hat{\mathbf{z}}. \quad (1c)$$

As shown in Fig. 1, it follows that

$$\hat{\mathbf{x}}_1 = -\hat{\mathbf{x}}_2 \quad \hat{\mathbf{y}}_1 = \hat{\mathbf{y}}_2 \quad \hat{\mathbf{z}}_1 = -\hat{\mathbf{z}}_2. \quad (2)$$

By convention a mirror's *yaw angle* α describes right-handed rotation about that mirror's $\hat{\mathbf{y}}$ axis, with each mirror's center of rotation coincident with the center of that mirror's reflecting surface.

For the remainder of this article we confine our attention to the planar motions shown in Fig. 1, *i.e.*, we omit translations along the $\hat{\mathbf{y}}$ axis (vertical translations) and also rotations about the $\hat{\mathbf{x}}$ axis (pitch rotations). Then a complete set of motional coordinates is $\{\alpha_1, \alpha_2, x_1, x_2, z_1, z_2\}$, where $\mathbf{x} = x_1\hat{\mathbf{x}}$ is the displacement of mirror 1 along the $\hat{\mathbf{x}}$ axis, *etc.*

By convention we assign a positive radius of curvature to concave mirrors. For $\{R_1, R_2\}$ the mirror radii, the well-known criterion for optical stability of a Fabry-Perot cavity is [4,5]

$$0 < g_1 g_2 < 1 \quad (3)$$

where

$$g_1 = 1 - L/R_1, \quad (4a)$$

$$g_2 = 1 - L/R_2. \quad (4b)$$

It follows that g_1 and g_2 must have the same sign:

$$\text{sign } g_1 = \text{sign } g_2 \equiv \text{sign } g. \quad (5)$$

The stability criterion (3) can also be shown to imply

$$\text{if } \text{sign } R_1 R_2 = 1$$

$$R_1 + R_2 > L$$

else

$$R_1 + R_2 < L. \quad (6)$$

These two inequalities allow us to express the one-way optical cavity length L in terms of the mirror centers $\{\mathbf{c}_1, \mathbf{c}_2\}$ as follows:

$$L = R_1 + R_2 - (\text{sign } R_1 R_2) |\mathbf{c}_1 - \mathbf{c}_2|, \quad (7)$$

without restriction on the signs of R_1 and R_2 . Strictly speaking the above expression has no meaning for flat mirrors, but our final results will also be valid in the limit $R \rightarrow \infty$. The cavity length is then explicitly given in terms of the displacements $\{\alpha_1, \alpha_2, x_1, x_2, z_1, z_2\}$ by

$$\begin{aligned} L = & R_1 + R_2 - \text{sign}(R_1 R_2) \\ & \times \left[(z_1 + z_2 + R_1 \cos \alpha_1 + R_2 \cos \alpha_2 - L)^2 \right. \\ & \left. + (x_1 + x_2 + R_1 \sin \alpha_1 + R_2 \sin \alpha_2)^2 \right]^{1/2}. \quad (8) \end{aligned}$$

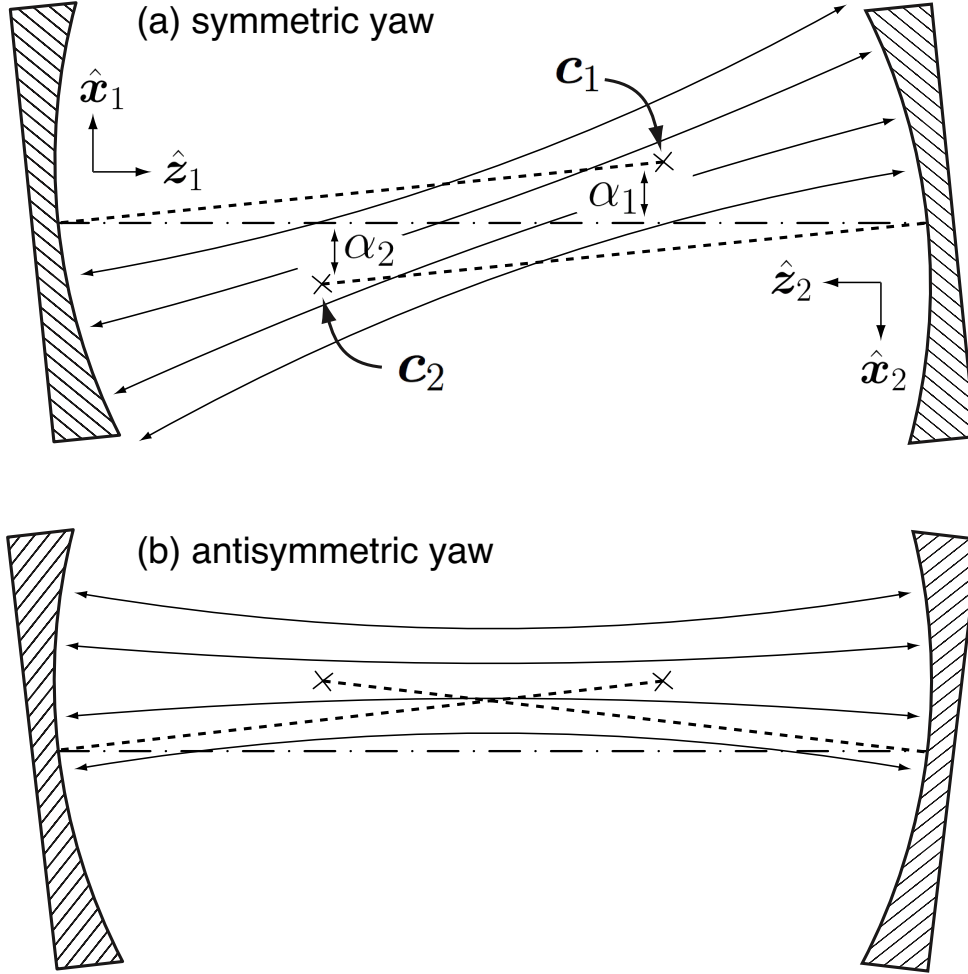


Fig. 1. Motion of mirrors in a Fabry-Perot cavity, and the consequent displacement of the mode axis. Due to light pressure, symmetric yaw motions (a) are statically stable, while antisymmetric yaw (b) is statically unstable. Here the mirrors' centers of curvature are $\{c_1, c_2\}$, the mirror yaw angles are $\{\alpha_1, \alpha_2\}$, and the mirror-specific basis vectors are $\{\{\hat{x}_1, \hat{z}_1\}, \{\hat{x}_2, \hat{z}_2\}\}$.

3 Virtual Work

For a non-degenerate cavity with reasonably high finesse \mathcal{F} , and for adiabatically slow mirror motions, we assume that the optical beam axis tracks the geometric cavity axis as depicted in Fig. 1. For the present we make this approximation purely on physical grounds; later on (see (32)) we will draw upon the modal analysis of Solimeno *et al.* to confirm that the corrections to the stiffness matrix resulting from this approximation are small.

Then for P the optical power reflected from each mirror, a change δL in the cavity length (8) is associated with mechanical work δW done on the cavity

according to

$$\begin{aligned} \delta W = -\frac{2P}{c} \delta L & \qquad \text{light pressure} \\ -F_{\text{stab}}(z_1 + z_2) & \qquad \text{stabilizing force} \end{aligned} \quad (9)$$

where c is the speed of light. Here we have included the work done by an externally-applied stabilizing force F_{stab} that holds the mirrors in position against the pressure of the light; we will calculate the required magnitude of F_{stab} shortly.

We allow the optical power to be an arbitrary function of the mirror coordinates, $P = P(\alpha_1, \alpha_2, x_1, x_2, z_1, z_2)$, but for compactness of notation we will suppress the arguments of P . It will turn out that the explicit functional form of P is not needed. The cavity length L too is a function of these same coordinates, and we *will* need to know the functional form of L , which was given in (8).

By convention, we have chosen the origin of our coordinate system such that when the cavity is in mechanical equilibrium $0 = \alpha_1 = \alpha_2 = x_1 = x_2 = z_1 = z_2$. Introducing the sum and difference coordinates

$$x_+ = x_1 + x_2 \qquad x_- = x_1 - x_2 \quad (10a)$$

$$z_+ = z_1 + z_2 \qquad z_- = z_1 - z_2, \quad (10b)$$

the expression (8) for L then implies that the following partial derivatives vanish:

$$0 = \frac{\partial L}{\partial \alpha_1} = \frac{\partial L}{\partial \alpha_2} = \frac{\partial L}{\partial x_+} = \frac{\partial L}{\partial x_-} = \frac{\partial L}{\partial z_-}. \quad (11)$$

To first order in these five displacements $\delta L = 0$ and so $\delta W = 0$ is assured. For the remaining displacement z_+ we have $\partial L / \partial z_+ = -1$, and so $\delta W = 0$ requires

$$F_{\text{stab}} = 2P/c. \quad (12)$$

Physically, F_{stab} is the force required to hold the mirrors stationary against light pressure.

Later on in our analysis, the longitudinal optical spring constant k will appear:

$$k = \frac{2}{c} \frac{\partial P}{\partial z_+} = \frac{2}{c} \frac{\partial P}{\partial z_1} = \frac{2}{c} \frac{\partial P}{\partial z_2}. \quad (13)$$

In contrast to all the other parameters of our analysis, the longitudinal spring constant cannot be determined from purely geometric arguments. The light pressure is a function of the finesse, and the state of resonance in the cavity. Thus, a comprehensive analysis of Fabry-Perot optical resonances is required, and in general k will turn out to depend on non-geometric parameters like the cavity finesse and tuning.

Fortunately, the torsional dynamics of the system—which are our main concern—will turn out not to depend on k , and so we will not need to specify the functional form of P .

4 The Stiffness Matrix

Given an arbitrary trajectory of the mirror coordinates, δW can be integrated to obtain the net work W done on the cavity mirrors. The increment δW is said to be *conservative* if W depends only on the end-point of the trajectories, such that $W = 0$ for all closed-loop trajectories. In this case W may be regarded as the effective potential energy of the mirror motion.

We now show that W is conservative for quasi-static mirror motions. Let \mathbf{q} be a vector of mirror displacements

$$\mathbf{q} = [\alpha_1, \alpha_2, x_+, x_-, z_+, z_-].$$

Along an arbitrary trajectory $\mathbf{q}(s)$ parametrized by $s \in (0, 1)$, we integrate (9) to obtain the net work W done on the mirrors:

$$W = \int \delta W = -\frac{2}{c} \int_0^1 ds P(\mathbf{q}(s)) \frac{\partial L(\mathbf{q}(s))}{\partial s} - F_{\text{stab}} \int_0^1 ds \frac{\partial z(s)}{\partial s}. \quad (14)$$

Here we have introduced the quasi-static assumption that the optical power is determined solely by the mirror coordinates, *i.e.* $P = P(\mathbf{q}(s))$.

We now expand W to second order in \mathbf{q} . The first-order terms cancel by virtue of the mechanical equilibrium condition (12), and the remaining second-order terms are

$$W = \sum_{i,j} -\frac{2}{c} \left[\frac{1}{2} P \frac{\partial^2 L}{\partial q_i \partial q_j} \int_0^1 ds \frac{\partial}{\partial s} q_i(s) q_j(s) + \frac{\partial P}{\partial q_i} \frac{\partial L}{\partial q_j} \int_0^1 ds q_i(s) \frac{\partial}{\partial s} q_j(s) \right]. \quad (15)$$

The key step in proving that W is conservative is showing that the second tensor in (15) is symmetric, *i.e.*, for T_{ij} defined by

$$T_{ij} \equiv \frac{\partial P}{\partial q_i} \frac{\partial L}{\partial q_j}, \quad (16)$$

we have to show $T_{ij} = T_{ji}$.

In proving symmetry, we have to accomodate nonzero values for the power derivatives $\partial P/\partial q_i$. Physically, these derivatives describe the dependence of the cavity power on mirror displacements. Such dependence can arise, *e.g.*, from mode mismatch created by mirror displacements. The virtual work analysis must recognize and accommodate this dependence.

However, even allowing arbitrary partial derivatives of P , the proof of symmetry is easy. From the equilibrium condition (11) and the definition of k (13), T is trivially symmetric because its sole nonzero component is

$$\frac{\partial P}{\partial z_+} \frac{\partial L}{\partial z_+} = -\frac{\partial P}{\partial z_+} = -\frac{ck}{2}, \quad (17)$$

where k is the optical spring constant introduced in (13). All other derivatives of L vanish by (11). This allows us to write W as:

$$W = -\frac{2}{c} \sum_{i,j} \left[\left(\frac{1}{2} P \frac{\partial^2 L}{\partial q_i \partial q_j} + \frac{1}{2} \frac{\partial P}{\partial q_i} \frac{\partial L}{\partial q_j} \right) \times \int_0^1 ds \frac{\partial}{\partial s} q_i(s) q_j(s) \right]. \quad (18)$$

The integral can be immediately evaluated to yield a net work W that explicitly depends only on the endpoint $\mathbf{q}(s=1)$, and which is therefore conservative:

$$W = -\frac{1}{c} \sum_{i,j} \left(P \frac{\partial^2 L}{\partial q_i \partial q_j} + \frac{\partial P}{\partial q_i} \frac{\partial L}{\partial q_j} \right) q_i(s) q_j(s) \Big|_{s=1}. \quad (19)$$

Reverting to tensor notation this is

$$W = \frac{1}{2} \mathbf{q} \cdot \boldsymbol{\kappa} \cdot \mathbf{q} + \frac{1}{2} k z_+^2. \quad (20)$$

The stiffness matrix $\boldsymbol{\kappa}$ can be evaluated in a form suitable for engineering use from (8), (13), and (19):

$$\boldsymbol{\kappa} = \frac{2P}{c(R_1 + R_2 - L)} \begin{bmatrix} 1 & R_1 & R_2 \\ R_1 & R_1(L-R_2) & R_1 R_2 \\ R_2 & R_1 R_2 & R_2(L-R_1) \end{bmatrix}. \quad (21)$$

The factor $(\text{sign } R_1 R_2)$ in (8) turns out to enter only as $(\text{sign } R_1 R_2)^2 = 1$, and hence it does not appear explicitly. Here $\boldsymbol{\kappa}$ is coupled to the displacement vector \mathbf{q}

$$\mathbf{q} = \begin{bmatrix} x_+ \\ \alpha_1 \\ \alpha_2 \end{bmatrix}. \quad (22)$$

Since W does not depend on x_- or z_- , these displacements are omitted from $\boldsymbol{\kappa}$ in (21) and from \mathbf{q} in (22).

Our sign conventions are such that positive eigenvalues of $\boldsymbol{\kappa}$ are associated with statically stable displacement eigenvectors, and negative eigenvalues with statically unstable displacement eigenvectors.

From a physical point of view, the stiffness matrix (21) seems overly simple. Why are important parameters like the cavity finesse and the cavity tuning not present? Basically, the analysis is for small motions around a stationary point on the optical axis and to first order the cavity length is not changed by lateral or torsional displacements. So even though the cavity power can depend in first order on lateral and/or torsional displacements (misaligned case), this power-dependency is not coupled to a cavity length change, and hence does no virtual work, and hence does not enter into the stiffness matrix.

5 The Long-Cavity Limit

Now we specialize our results to suspended cavities with length $L \gg d_M$, where d_M is the mirror diameter. In long cavities the dynamics of the suspended mirrors are dominated by the terms in $\boldsymbol{\kappa}$ that couple to the yaw angles α_1 and α_2 , while the terms that couple to the transverse mirror displacement x_+ are suppressed by one or more powers of d_M/L .

This leads us to define a *torsional stiffness matrix*

$$\bar{\boldsymbol{\kappa}} = \frac{2P}{c(R_1 + R_2 - L)} \begin{bmatrix} R_1(L - R_2) & R_1R_2 \\ R_1R_2 & R_2(L - R_1) \end{bmatrix} \quad (23)$$

that has SI units of $\text{N} \cdot \text{m}/\text{radian}$. By definition, $\bar{\boldsymbol{\kappa}}$ couples only to the yaw displacements $\mathbf{q} = [\alpha_1, \alpha_2]$, and thus describes the purely torsional stiffness of the mirrors.

In terms of g_1 and g_2 , as defined in (4), $\bar{\boldsymbol{\kappa}}$ is particularly simple

$$\bar{\boldsymbol{\kappa}} = \frac{2PL}{c(1 - g_1g_2)} \begin{bmatrix} -g_2 & 1 \\ 1 & -g_1 \end{bmatrix}. \quad (24)$$

We see that the stiffness matrix is a smooth function of g_1 and g_2 , and hence a smooth function of $1/R_1$ and $1/R_2$, such that cavities in which one mirror is flat or has negative curvature are accommodated by analytic continuation.

The determinant of the stiffness matrix is

$$\det\left(\frac{c\bar{\boldsymbol{\kappa}}}{2PL}\right) = -(1 - g_1g_2)^{-1} \quad (25)$$

which is seen to be negative for all optically stable cavities. Recalling that the determinant of a matrix is the product of its eigenvalues, we see that $\bar{\boldsymbol{\kappa}}$ always

has one positive and one negative eigenvalue, whose geometric mean satisfies $|\det \bar{\kappa}|^{1/2} \geq 2PL/c$.

It follows that whatever the design of the optical cavity, no suspended-mirror Fabry-Perot cavity can be entirely free of torsional stiffness effects. In particular, a statically unstable torsional mode will always be present.

Seeking further insight, we recall that within a Fabry-Perot cavity formed by spherical mirrors the beam intensity profile $I(x, y)$ is a Gaussian function whose width is conventionally described in terms of a spot size w :

$$I(x, y) = \frac{2P}{\pi w^2} e^{-2(x^2+y^2)/w^2}. \quad (26)$$

The spot sizes w_1 and w_2 on the two cavity mirrors are related to the mirror parameters g_1 and g_2 by [5]

$$w_1^2 = \frac{\lambda L}{\pi} \left[\frac{g_2}{g_1(1 - g_1 g_2)} \right]^{1/2} \quad (27a)$$

$$w_2^2 = \frac{\lambda L}{\pi} \left[\frac{g_1}{g_2(1 - g_1 g_2)} \right]^{1/2} \quad (27b)$$

which can be inverted to yield

$$g_1 = \pm \frac{w_2}{w_1} \left[1 - \frac{w_0^4}{w_1^2 w_2^2} \right]^{1/2} \quad (28a)$$

$$g_2 = \pm \frac{w_1}{w_2} \left[1 - \frac{w_0^4}{w_1^2 w_2^2} \right]^{1/2} \quad (28b)$$

where

$$w_0 = \sqrt{L\lambda/\pi}. \quad (29)$$

The previous criterion for optical stability (3) can be shown to imply

$$w_1 w_2 \geq w_0^2. \quad (30)$$

Thus w_0 is the smallest possible geometric mean of the two spot diameters.

In order to accommodate larger optical power and in order to minimize thermal noise terms[2,3] one will try to set the spot size on the mirrors as large as possible. Setting $w = w_1 = w_2$ and assuming $w \gg w_0$ one can expand $\bar{\kappa}$ in powers of w_0^4/w^4 . To leading order the eigenvalues are then given by

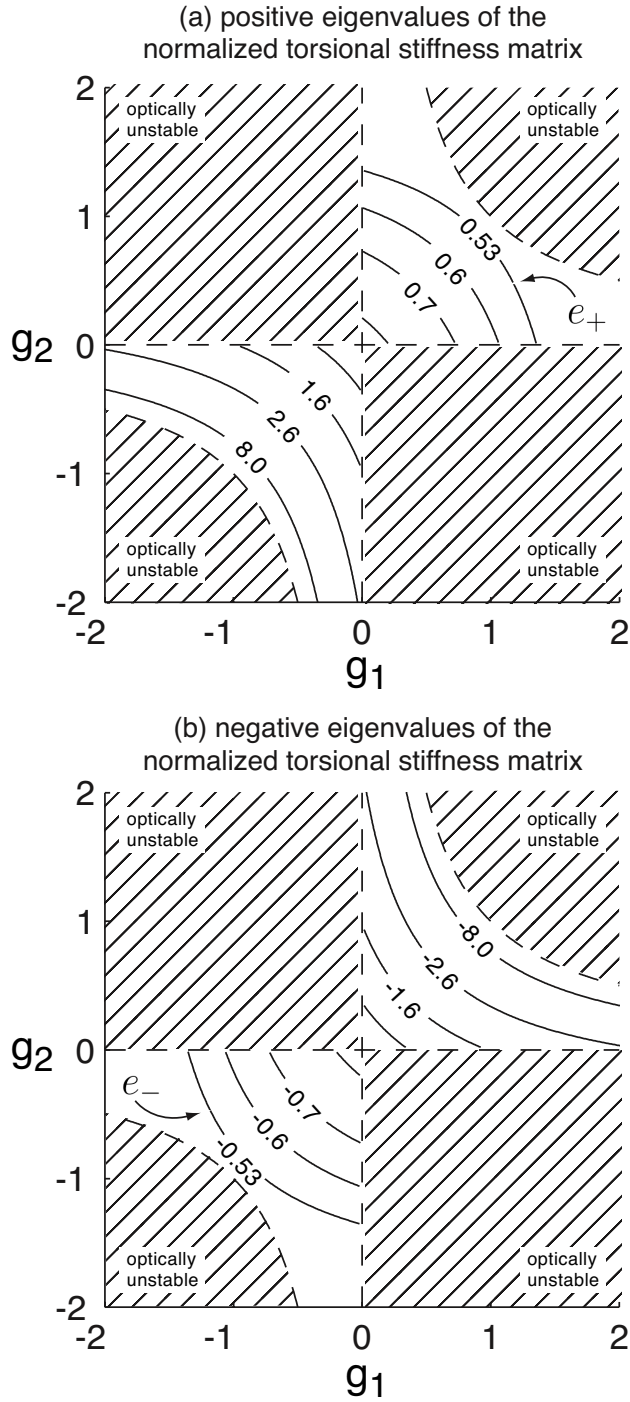


Fig. 2. Eigenvalues of the torsional stiffness matrix. The nondimensional matrix $c\bar{\kappa}/(2LP)$ is depicted, with (a) showing contours of constant positive eigenvalue e_+ and (b) showing contours of constant negative eigenvalue e_- . By (24), these satisfy $e_+e_- = -(1-g_1g_2)^{-1}$. Negative eigenvalues are associated with the statically unstable symmetric yaw depicted in Fig. (1)(b). Torsional instability is seen to be least strong in the region $g_1 \sim g_2 \sim -1$.

$$\kappa_{\text{major}} \simeq \mp \frac{LP}{c} \frac{4w^4}{w_0^4}, \quad (31a)$$

$$\kappa_{\text{minor}} \simeq \pm \frac{LP}{c}. \quad (31b)$$

where the negative solution for κ_{major} and the positive solution for κ_{minor} are associated with positive g -parameters. The above approximation holds for a range of beam sizes $w \gg w_0$ as long as none of the higher order transverse modes becomes resonant. We see that a large spot size is directly linked to large torsional stiffness, such that the dominant eigenvalue is statically stable if and only if $\text{sign } g = -1$.

6 Comparison with Modal Analysis

In their modal analysis Solimeno *et al.* give a general expression [1, eq. 66] for the optomechanical torque acting on a single mirror, and from this result the diagonal element $\bar{\kappa}_{11}$ of the torsional stiffness matrix can be calculated. We now carry through this calculation, and we show that the predicted torsional stiffness agrees precisely with (24). Also, we calculate the corrections due to finite cavity finesse and off-resonance tuning, and we show that these corrections are small.

Adopting the notation of Solimeno *et al.*, we define χ to be the two-way optical phase of the cavity, such that $\chi = 0 \pmod{2\pi}$ for on-resonance tuning. For \mathcal{F} the cavity finesse, we restrict our attention to near-resonance tunings, such that $\chi \sim \mathcal{O}(\mathcal{F}^{-1})$. Then starting from [1, eq. 66], and making successive use of eqs. (67c, 68, 15, 67ff, 26, 2, and 13) of [1], then expanding to leading and next-to-leading order in \mathcal{F}^{-1} and χ , and expressing the results in terms of g_1 and g_2 via (27ab), we arrive at the following modal prediction:

$$\bar{\kappa}_{11} = \frac{-2PLg_2}{c(1 - g_1g_2)} \times \left[1 - \frac{\pi^2}{(1 - g_1g_2)\mathcal{F}^2} - \frac{\chi \text{sign } g}{2(g_1g_2(1 - g_1g_2))^{1/2}} \right]. \quad (32)$$

The leading term agrees exactly with our geometric result (24). The effects of finite cavity finesse and off-resonance tuning are seen to be small, respectively $\mathcal{O}(\mathcal{F}^{-2})$ and $\mathcal{O}(\chi)$, as was previously assumed on physical grounds.

In obtaining this result we modified the calculations of Solimeno *et al.* in one respect. In accord with Milloni and Eberly [5], we altered the phase ϕ defined in

[1, eq. 13] to be $\phi = \arccos(\sqrt{g_1 g_2} \text{ sign } g)$ instead of $\phi = \arccos(\sqrt{g_1 g_2})$. Without this modification the sign of the torsional spring for negative- g cavities is wrong. Furthermore, by computing the diagonal terms only the importance of the coupling between the two cavity mirrors has been missed. We will see in the next section that this alteration has significant engineering implications.

7 Worked Examples and Discussion

As examples, we consider the current LIGO interferometer [6,7] as well as a recent reference design for an next-generation high-power LIGO interferometer [8]. LIGO cavities have a length $L = 4$ km. The light source in both cases is a Nd:YAG laser that operates at $\lambda = 1064$ nm. The design specifies an intracavity power of $P = 15$ kW for current LIGO and $P = 830$ kW for advanced LIGO. In the current detector the two cavity mirrors have radii of curvature $R_1 = 7.4$ km and $R_2 = 11.6$ km, respectively. For Advanced LIGO a desirable beam spot size from the standpoint of thermal noise is $w_1 = w_2 = 6$ cm, which by (4) and (28) implies $R_1 = R_2 = 54.4$ km for positive- g mirrors, or $R_1 = R_2 = 2.076$ km for negative- g mirrors.

Table 1 summarizes these design parameters and gives the optical torsional stiffness eigenvalues for both designs. For purposes of comparison an estimated torsional pendulum stiffness of the suspended mirrors is listed as well. This pendulum stiffness is estimated as follows. LIGO uses fused silica mirrors with a diameter of $d_M = 25$ cm and a thickness of $t = 10$ cm; this gives a weight of $M \sim 10.8$ kg. Advanced LIGO calls for sapphire substrates with a diameter of $d_M = 31.4$ cm, a thickness of $t = 13$ cm and a weight of $M \sim 40$ kg. In both cases we assume that the suspension's fundamental torsional frequency is $f \sim 0.5$ Hz. This yields the approximate pendulum stiffnesses given in Table 1. It should be kept in mind that giving a single number for the pendulum stiffness

Table 1

Cavity parameters and stiffness values for current LIGO and the Advanced LIGO design.

parameter	LIGO	advLIGO	unit
P	15	830	kW
g_1	0.460	± 0.927	–
g_2	0.726	± 0.927	–
κ_{pendulum}	~ 0.51	~ 3.0	N·m
κ_{major}	-0.96	∓ 301	N·m
κ_{minor}	0.25	± 11.5	N·m

presents a somewhat simplified picture of the mirror suspension mechanisms, which actually have multiple torsional modes.

The most striking feature of this table is the startlingly large major eigenvalue of the torsional stiffness matrix for Advanced LIGO. On purely dimensional grounds a much smaller eigenvalue might have been expected, of order $LP/c \sim 11 \text{ N} \cdot \text{m}$ (*i.e.*, the same order as the minor eigenvalue). However, this natural torque scale is multiplied by a dimensionless factor that scales as the fourth power of the beam spot size: $4(w/w_0)^4 \sim 4(6/3.68)^4 \sim 28$. For both designs, when the detector operates at full power, the statically unstable mode of the optical spring dominates the restoring torque of the mirror suspension.

For current LIGO the optical spring is weak enough that it can be compensated by the auto-alignment system [9] without major changes to the feedback control system. For Advanced LIGO further analysis is needed, but by adopting negative g -parameters for the mirrors, such that the dominant torsional stiffness eigenvalue κ_{major} is positive, the dominant torsional mode might be made statically stable—even strongly self-aligning—in pitch and yaw. The auto-alignment system should then be made strong enough to compensate for the unstable κ_{minor} . Since the auto-alignment system relies on the cavities to be on-resonance, a reasonable strategy might be to lock at low power, engage the auto-alignment system and then turn the input power up. This will require the design of mirror suspension controllers that can adapt to the changing dynamics of the mirrors during the power-up.

It should be kept in mind that our analysis is quasi-static. A more complete analysis would include the time-lag as the cavity light responds to mirror motion displacements, along the lines of the modal formalism of Solimeno *et al.* [1]. One should also keep in mind that gravitational-wave detectors are much more sophisticated than a simple cavity—usually consisting of multiple coupled resonators built around a Michelson interferometer. These systems will require considerable further analysis to fully elucidate the trade-offs attendant to the simultaneous interferometric goals of large optical power, large beam diameter, and stable mirror suspension.

In summary, we have shown that high power Fabry-Perot cavities form an optical torsion spring that couples the two cavity mirrors. In all cases, there is one stable and one unstable torsional mode. In interferometric gravitational wave detectors using high optical powers, the torsional stiffness of these optical springs can be much larger than the torsional stiffness of the mirror suspensions, and must be taken into account in the system design.

Acknowledgements

The LIGO Observatories were constructed by the California Institute of Technology and Massachusetts Institute of Technology with funding from the National Science Foundation under cooperative agreement PHY-9210038. The LIGO Laboratory operates under cooperative agreement PHY-0107417. This paper has been assigned LIGO Document Number LIGO-P030055-B.

One of the authors (JAS) acknowledges the support of the NIH, the NSF, and the DARPA 3D Atomic Resolution Imaging Program, all of which help support the University of Washington's Quantum System Engineering Laboratory.

References

- [1] S. Solimeno, F. Barone, C. De Lisio, L. Di Fiore, L. Milano, and G. Russo, “*Fabry-Perot resonators with oscillating mirrors*,” *Physical Review A* 43(11), 6227–6240 (1991).
- [2] V. B. Braginsky, M. L. Gorodetsky, and S. P. Vyatchanin, *Phys. Lett. A* 264, 1 (1999).
- [3] M. M. Fejer, S. Rowan, G. Cagnoli, D. R. M. Crooks, A. Gretarsson, G. M. Harry, J. Hough, S. D. Penn, P. H. Sneddon, and S. P. Vyatchanin, “*Thermoelastic dissipation in inhomogeneous media: Loss measurements and displacement noise in coated test masses for interferometric gravitational wave detectors*,” submitted to *Phys. Rev. D*.
- [4] O. Svelto, *Principles of Lasers*, Plenum Press, 1989.
- [5] P. W. Milonni and H. H. Eberly, *Lasers*, John Wiley & Sons, 1988.
- [6] A. Abramovici, W. E. Althouse, R. W. P. Drever, Y. Gursel, S. Kawamura, F. J. Raab, D. Shoemaker, L. Sievers, R. E. Spero, K. S. Thorne, R. E. Vogt, R. Weiss, S. E. Whitcomb, and M. E. Zucker, “*LIGO—the laser interferometer gravitational-wave observatory*,” *Science* 256, 325–333 (1992).
- [7] B. Barish and R. Weiss, “*LIGO and the Detection of Gravitational Waves*,” *Phys. Today* 52 (Oct), 44 (1999).
- [8] D. Shoemaker, “*Advanced LIGO: Context and Overview (Proposal to the NSF)*,” Technical report, LIGO project, document M030023-00-M (2003).
P. Fritschel, “*Second generation instruments for the Laser Interferometer Gravitational-Wave Observatory (LIGO)*,” *Proceedings of the SPIE—The International Society for Optical Engineering*, Vol. 4856, 282–91 (2003).
- [9] P. Fritschel, N. Mavalvala, D. Shoemaker, D. Sigg, M. Zucker, and G. Gonzalez, “*Alignment of an interferometric gravitational wave detector*” *Appl. Opt.* 37, 6734–6747 (1998).